Application of Magnus series for polarization evolution in fibers

N. Korneev

Instituto Nacional de Astrofísica, Óptica y Electrónica,
Apt.Postal 51 y 216 , CP 72000, Puebla, Pue., Mexico.
e-mail korneev@inaoep.mx

We apply the technique of Magnus series to build approximations for polarization evolution in fibers with varying twist and birefringence. Conditions for trajectory mixing on Poincaré sphere are identified. The technique relates realistic perturbation parameters to the parameters of popular coarse step method of numerical simulation. We demonstrate that liner polarization mode dispersion, if it is a dominant process, leads for big propagation lengths to a speckle-like output pulse shape.

Keywords: Polarization; optical fibers; pulse propagation.

La serie de Magnus se aplica para obtener las expresiones aproximadas para la evolución de la polarización de luz en una fibra óptica con torsión y birrefrigencia aleatorias. Se identefican las condiciones para que la trayectoria cubre la esfera de Poincaré. Los parámetros reales de perturbación se relacionan con los parámetros del método de divisiones grandes, que se utiliza para modelos numéricos. Mostramos, que la dispersión modal de polarización, cuando es el proceso dominante, produce el pulso del tipo speckle temporal.

Descriptores: Polarización; fibras ópticas; propagación de pulsos.

PACS: 42.81.-i; 42.81.Gs

1. Introduction

Optical fibers are practically always birefringent. Typical beat lengths range from millimeters to tens of meters, and there are random additions to birefringence and polarization rotations induced by fiber imperfections and strains [1]. The usual combination of relatively strong birefrigence and random variations of the birefringence and twist presents particular difficulties for analysis. In this case the solution for amplitude of polarization mode is a rapidly oscillating function with slowly varying magnitude and phase. One practically important technique widely used for simulations, and generally consistent with the experiment is called the coarse step method [2]. It assumes that the fiber is made of pieces with constant birefringence separated by random polarization elements. Of course, it is difficult to expect that real perturbations in fibers have this character. In fact, fitting parameters are used to compare the theory and the experiment. Measurements of fiber birefringence distributions have been refined recently [3,4], and it is desirable to establish the validity range of coarse step model and relate it to the realistic perturbation.

In this paper we suggest the perturbation method which is well suited for the situation of strong average birefringence with relatively small variations in birefringence and twist. It is based on the mathematical technique investigated in detail in recent publications of Iserles and Nørsett [5] devoted to the numerical solution of differential equations. Their work is based on the earlier article by Magnus [6]. Accordingly, the authors call it the Magnus series technique. The method permits to separate the exactly integrable part and then to obtain successive approximation terms proportional to the powers of perturbation. The terms are conveniently expressed as diagrams. For the case of fibers, the series converge rapidly for lengths comparable to the beat length of perturbation, thus the behavior of solution can be predicted for many beat lengths of the main part of birefringence. The method, apart from its utility for numerical calculation, gives useful insights on the factors which influence the polarization behavior. In particular, we will obtain conditions for spreading of the trajectory over Poincaré sphere and estimate the rate of this spreading. Good analytical approximations can be suggested for the case of periodic perturbations. We will also show that the coarse step model can be valid for a wide variety of perturbation types, and relate the parameters of this model to the real parameters of perturbation. We also investigate the shape of linear pulse in a fiber with dominant polarization mode dispersion.

2. Outline of Magnus series technique

The polarization evolution in fibers is described by two coupled ordinary differential equations

$$\frac{d\mathbf{S}}{dz} = \mathbf{A}(z)\mathbf{S}, \tag{1}$$

where $\mathbf{S}$ is a two-component vector of complex amplitudes, and $\mathbf{A}$ is the anti-Hermitian 2×2 complex matrix ($\mathbf{A}^T = -\mathbf{A}^*$, or $\mathbf{A} = i\mathbf{B}$, where $\mathbf{B}$ is Hermitian). The abstract solution can be written in the form

$$\mathbf{S}(z) = \mathbf{U}(z)\mathbf{S}(0) \tag{2}$$

with unitary 2×2 matrix $\mathbf{U}$ (Jones matrix). All such matrices form a Lie group [7], and $\mathbf{U}$ can be represented as the matrix exponential

$$\mathbf{U}(z) = \exp(\mathbf{Q}(z)), \tag{3}$$

where a matrix $\mathbf{Q}(z)$ is anti-Hermitian. The basis in the space of Hermitian 2×2 matrices is given by Pauli matrices:

$$\mathbf{I} = \left[\begin{array}{cc} 1 & 0 \\ 0 & 1 \end{array} \right],$$

$$\sigma_1 = \left[\begin{array}{cc} 0 & 1 \\ 1 & 0 \end{array} \right], \sigma_2 = \left[\begin{array}{cc} 0 & -i \\ i & 0 \end{array} \right], \sigma_3 = \left[\begin{array}{cc} 1 & 0 \\ 0 & -1 \end{array} \right] \quad (4)$$

Any matrix $\mathbf{A}$ can be represented as

$$\mathbf{A} = i(g_0(z)\mathbf{I} + g_1(z)\sigma_1 + g_2(z)\sigma_2 + g_3(z)\sigma_3), \quad (5)$$

with real scalar functions g_j. The commutation relations for Pauli matrices are

$$[i\sigma_n, i\sigma_m] = -2i\varepsilon_{jnm}\sigma_j, \quad (6)$$

with the antisymmetric tensor ε_{jmn}. The idea of the Magnus series method is to write $\mathbf{Q}(z)$ from Eq.(3) in terms of $\mathbf{A}(z)$.

The Magnus series is

$$\mathbf{Q}(z) = \int_0^z \mathbf{A}(z')dz' + \frac{1}{2}\int_0^z [\mathbf{A}(z'), \int_0^{z'}\mathbf{A}(z'')dz'']dz'$$

$$+ \frac{1}{4}\int_0^z [\mathbf{A}(z'), \int_0^{z'}[\mathbf{A}(z''), \int_0^{z''}\mathbf{A}(z''')dz''']dz'']dz'$$

$$+ \frac{1}{12}\int_0^z [[\mathbf{A}(z'), \int_0^{z'}\mathbf{A}(z'')dz''], \int_0^{z'}\mathbf{A}(z'')dz'']dz' + \ldots, \quad (7)$$

i.e. the expression for $\mathbf{Q}$ is obtained in terms of integrals and commutators multiplied by numeric coefficients. The exact structure of terms can be expressed by a diagrams. The order of term is equal to the number of $\mathbf{A}$'s in the expression. We will not use terms beyond the third order in this paper.

The complete series with the representation of terms as diagrams can be found in Ref. 5. The number of terms and their complexity grows rapidly with the order. The important theorem on the series convergence range is given in Ref. 5 (Theorem 8). It guarantees that if the matrix $\mathbf{A}$ Euclidian norm is less than ρ, the series converge at least for $z < 1/(8\rho)$. Thus, practically, the trade-off has to be found between validity range of approximation and its complexity.

For the polarization evolution task the underlying group is that one of unitary matrices $U(2)$, and it can be reduced to $SU(2)$ (unitary matrices with the determinant equal to unity). This is done by taking into account the phase shift common for two polarizations. Using $\mathbf{S}(z) = \exp(i\int_0^z g_0(z')dz') \cdot \mathbf{S}'(z)$, we obtain for $\mathbf{S}'(z)$ evolution the matrix $\mathbf{A}$ for which $g_0 = 0$. For the subsequent analysis we will directly utilize the representation Eq.(5) with $g_0 = 0$ and commutation relations Eq.(6) specific for $SU(2)$ group.

The usual method to visualize polarization states is the Poincaré sphere. Three real coordinates $x_j = \mathbf{S}\sigma_j\mathbf{S}^*$ are introduced. It is easy to demonstrate that with a proper normalization of input amplitudes, $\sum_j x_j^2 = 1$, thus it is possible to associate the polarization state with a point on the sphere.

The vector of coefficients $g_{1,2,3}$ in the $\mathbf{Q}$ representation by Pauli matrices Eq.(5) corresponds to an axis of rotation of the sphere. The rotation angle is proportional to the vector length.

We will use for $\mathbf{Q}$ the representation

$$\mathbf{Q}(z) = i\left(\sum_j \kappa_j^1(z)\sigma_j + \sum_j \kappa_j^2(z)\sigma_j + \ldots \right), \quad (8)$$

where coefficients $\kappa_j^p(z)$ correspond to the diagrams of the p-th order.

3. Application to a birefringent fiber with twist

To apply the technique successfully, it is necessary to extract from the matrix $\mathbf{A}$ the big principal part. This is easily done for example, if $\mathbf{A}$ is nearly constant or if the off-diagonal elements are much smaller than the diagonal ones. Physically, it can mean that we have, for example, nearly constant birefringence with relatively small variations in both birefringence and twist. The trajectory on the Poincaré sphere in this case corresponds mainly to the point rotation around the 3-rd axis, but both simulations and experiment demonstrate that due to the perturbations, after sufficiently big propagation length the trajectory will cover all the sphere.

Let us consider the case when there is a birefringent fiber with small additions to birefringence and twist. Then the right-hand side of Eq.(1)is [8]

$$\mathbf{A} = i\left[\begin{array}{cc} b_0 + b_3(z) & b_1(z) \\ b_1(z) & -b_0 - b_3(z) \end{array} \right]. \quad (9)$$

Here b_0 is the main part of the birefringence, and $b_{1,3}(z)$ are small real functions: $|b_0| >> |b_1(z)|, |b_3(z)|$.

The direct application of Magnus series is not highly useful: we will get approximations which are valid for the length of an order of $1/b_0$, *i.e.* of the order of the beatlength due to the main part of the birefringence. But it is possible to diminish the norm of the matrix by introducing the rotating basis $\mathbf{S}'$:

$$\mathbf{S} = \left[\begin{array}{cc} \exp(ib_0z) & 0 \\ 0 & \exp(-ib_0z) \end{array} \right] \mathbf{S}' = \mathbf{E}(z)\mathbf{S}'. \quad (10)$$

For $\mathbf{S}'$ the equation is $\frac{d\mathbf{S}'}{dz} = \mathbf{A}'(z)\mathbf{S}'$ with

$$\mathbf{A}' = i\left[\begin{array}{cc} b_3(z) & b_1(z)\exp(-2ib_0z) \\ b_1(z)\exp(2ib_0z) & -b_3(z) \end{array} \right] \quad (11)$$

and now all matrix elements are small, and the Magnus series convergence is guaranteed for lengths having the order of the beat length for perturbation $l \cong 1/\max(|b_{1,3}|)$. Now, the functions in the Eq. (5) are: $g_1(z) = b_1(z)\cos(2b_0z)$, $g_2(z) = b_1(z)\sin(2b_0z)$, $g_3(z) = b_3(z)$. In the first order of perturbation,

$$\kappa_j^1(z) = \int_0^z g_j(z')dz'$$

The integrals for $\kappa_{1,2}^1(z)$ give rapidly varying and small terms if $b_1(z)$ does not contain spatial harmonics with wavenumber close to $2b_0$. "Close" means in our context that their spatial frequency k must approximately fall into the interval $2b_0 - \max(|b_1|) < k < 2b_0 + \max(|b_1|)$. In this case the value of $\kappa_{1,2}^1(z)$ can approach unity in the validity range for the approximation l. Thus, the matrix $\exp(\mathbf{Q}(z))$ which describes the behavior of $\mathbf{S}'$ corresponds on the Poincaré sphere to the combination of two movements: rapid and small "jitter" and the relatively slow rotation for big angle. The total trajectory on the sphere for given initial polarization is obtained by applying the matrix of Eq.(10) to the vector $\exp(\mathbf{Q}(z))\mathbf{S}'(0)$. The "slow and big " terms of $\exp(\mathbf{Q}(z))$ act as initial conditions for the fast rotation given by Eq.(10), thus the trajectory spreads over the Poincare sphere. The result that the perturbation component with the spatial frequency $2b_0$ is responsible for mode coupling is well known, mainly in its statistical formulation [1], though limits of its application are somewhat unclear. $\kappa_3^1(z)$ simply gives an addition to birefringence.

The second order terms are given by

$$\kappa_j^2(z) = -\varepsilon_{jmn}\int_0^z g_m(z')\kappa_n^1(z)dz'$$

$$= -\varepsilon_{jmn}\int_0^z g_m(z')\int_0^{z'} g_n(z'')dz''dz', \quad (12)$$

$\kappa_3^2(z)$ is proportional to b_1^2, it is the second-order correction to the birefringence. The terms $\kappa_{1,2}^2(z)$ include the product b_1b_3, and they give the spreading on the Poincaré sphere if b_1 and b_3 contain spatial frequencies that add to $2b_0$. This factor can be important in comparison with the first-order term if the perturbation has the spectrum, which is small at the $2b_0$ spatial frequency, but has strong components in low or high-frequency domains. Thus, even if perturbations do not have spatial frequencies close to the $2b_0$, the spreading will occur because of the higher order processes. The rate of spreading,

though, will be proportional for the p-th order process to b^p.

For demonstration, we have performed a numerical calculation of the trajectory on the Poincaré sphere for the case when the additions to birefringence and twist have differnt periods $b_{1,3}(z) = \beta_{1,3}\cos(k_{1,3}z)$. The Eq.(11) was solved numerically for $b_0 = 1$, $\beta_{1,3} = 0.1$, propagation length 5000, and different relations between perturbation spatial frequencies k_1 and k_3. In general case (Fig.1a), when $k_1 + k_3$ are not close to $2b_0$ (we have taken $k_1 = 0.55, k_3 = 1.3$), the dominant accumulating effect is the second-order addition to birefringence, and the trajectory does not fill the sphere. When two frequencies add to a value close to $2b_0$ ($k_1 = 0.702, k_3 = 1.3$), the spreading occurs (Fig.1b). The strongest spreading is obtained when the coupling is produced by a first order term ($k_3 = 2.02$), $\beta_1 = 0$). It is presented in Fig.1c.

To compare the results obtained with the diagram technique with exact solutions we have chosen a simple example of a periodical perturbation $b_1(z) = \beta_1 \exp(2ik_0z)$. The terms of the 1-st to 3-rd order for this case are easily obtained analytically. The resulting expressions are rather big, so we do not reproduce them here. We have chosen for our simulation $b_0 = 10$, $\beta = 0.1$ and the length $l = 10$. The numerical solution of the Eq.(9) was calculated to the absolute exactitude 10^{-5} with a Matlab computer program, which uses the Runge-Kutta algorithm of 4-5 order. The absolute value of the maximal difference between the exact and approximate solutions in this interval is presented as a function of the perturbation frequency. It is seen, that the worst agreement is for the nearly resonance condition, but even there the approximation is adequate. Far from resonance, the terms of the first to third order give an error of approximately 10^{-4}. The perturbation terms seemingly converge at least for the range 10, which is more than the guaranteed range of convergence. It can be noted that the convergence theorem gives the lower limit for the range, and the range can be bigger for particular cases.
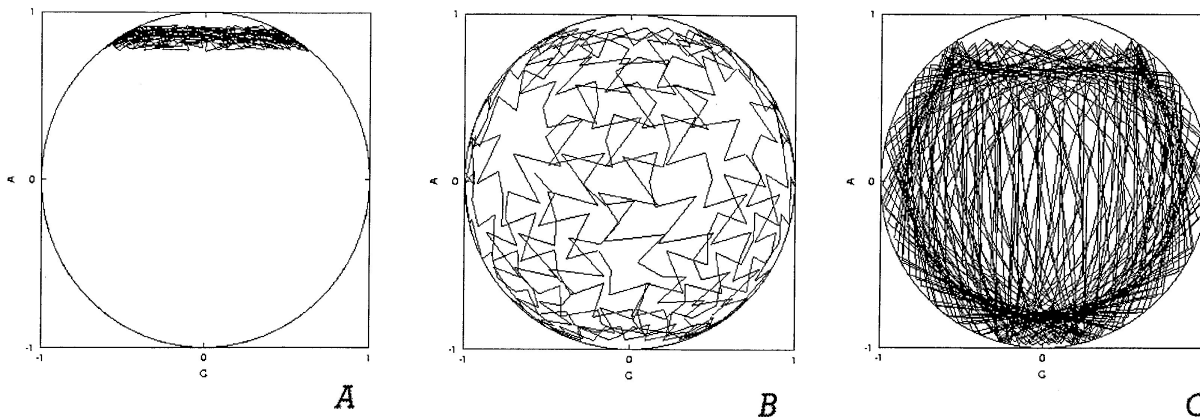

FIGURE 1 Examples of trajectory spreading on the Poincaré sphere. 400 points of every trajectory connected with straight lines are shown. A - the perturbation is far from resonance conditions, B - two different spatial frequencies in the perturbation spectrum sum to the characteristic spatial frequency of beatlength, C - one of the spatial frequencies is close to the characteristic spatial frequency of beatlength.
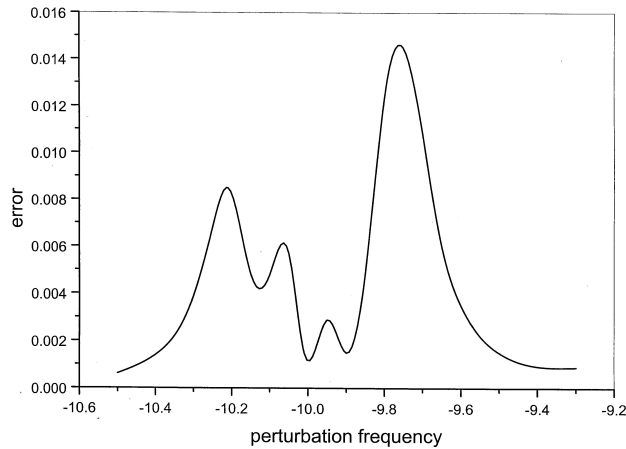
FIGURE 2 Example of the maximal difference between the exact value of the amplitude and the approximation with 4 terms of perturbation series. The amplitude itself has a characteristic absolute value of an order of unity and it has about 15 periods of oscillation in the interval. Details can be found in the text.

Trying to perform a Matlab calculation for the same length and $b_0 = 100$ on a modern personal computer was already resulting in difficulties - tens of minutes of calculation time and instabilities leading to the shutdown of the program by the operating system. Thus, the calculation with diagrams can be highly useful if the perturbation is small in comparison with the main birefringence.

The diagram technique justifies the widely used "ad hoc" method of numerical modeling of randomly birefringent fibers [3]. For modeling it is assumed that the fiber consists of pieces with constant birefringence, but there is abrupt random change of polarization state between two adjacent pieces. Though it does not seem probable that the perturbation in real fibers has this character, the model can be justified by the following argument. As the matrix, which describes the propagation at the distance of an order of perturbation beatlength $l = 1/\max(|b_{1,3}|)$ is given by the combination

$$\mathbf{U}(l) = \mathbf{E}(l)\exp(i\mathbf{Q}(l)), \tag{13}$$

the propagation at a distance Nl is given by a product of matrices

$$\mathbf{U}(Nl) = \mathbf{E}(l)\exp(i\mathbf{Q}_N(l))...\mathbf{E}(l)\exp(i\mathbf{Q}_1(l)), \tag{14}$$

where $\mathbf{E}(l)$ from the Eq.(10) formally correspond to the propagation in the uniformly birefringent fiber, and $\exp(i\mathbf{Q}_j(l))$ are determined by diagram terms, *i.e.* by the exact character of the perturbation. Nevertheless, if the frequency dependence of coefficients is taken into account (for example, by suggesting, as in Ref. 8 that $b_3(\omega, z) = \beta\omega$), it is seen that the matrices $\exp(i\mathbf{Q}_1(l))$ are generally frequency-dependent. It means that for the coarse steps model the polarization element inserted between two pieces of birefringent fiber performs frequency-dependent polarization transformation. More important, than the justification of the technique, is the possibility to relate by diagrams the perturbation statistics to the statistics of matrices $\exp(i\mathbf{Q}_j(l))$. If only the first

term in perturbation series is important, the main contributions to matrix elements are related to the Fourier harmonics of perturbation with the spatial frequency $2b_0$. If the perturbation is random, and its correlation length is smaller than the approximation validity range l, it seems quite probable that the matrices $\exp(i\mathbf{Q}_j(l))$ will uniformly sample the space. They will give a random rotation around the random axis on the Poincaré sphere.

4. Linear pulse propagation in a randomly birefringent fiber

The influence of random birefringence on pulse behavior is traditionally analyzed with a concept of differential delay, introduced in works of Poole and co-workers [9,10] . A wide pulse with limited spectrum splits in two components with well-defined polarization states and different propagation constants. If the big frequency range is spanned, the difference in propagation constants has statistical distribution. If the spectrum is wide, the ensemble over many realizations of fiber is taken. The analysis gives, that after the averaging for big propagation lengths the output pulse intensity has Gaussian shape. Its width is proportional to a square root of the propagation length.

The statistical analysis does not tell which shape individual pulses entering the statistical ensemble have. Intuitively, one can choose between two possibilities. The first one is that *every* individual pulse is nearly Gaussian. The second is that individual pulses have complicated shapes, but average to a smooth curve.

To anticipate the answer, we transform the Eq. (14). First, let us choose the central frequency ω_0 and the length l such, that $exp(ib_0l)$ entering $\mathbf{E}(l)$ is equal to 1. Then by a simple transformation the equation (14) is reduced to a form

$$\mathbf{U}_0\mathbf{U}_N^{-1}\mathbf{E}_\delta\mathbf{U}_N...\mathbf{U}_1^{-1}\mathbf{E}_\delta\mathbf{U}_1, \tag{15}$$

where $\mathbf{E}_\delta$ is a diagonal matrix with elements $\exp(\pm C\delta\omega)$, with $\delta\omega = \omega - \omega_0$, and unitary matrices $\mathbf{U}_i$ are such that $\mathbf{U}_1 = \exp(i\mathbf{Q}_1(l))$, $\mathbf{U}_2 = \exp(i\mathbf{Q}_2(l))\mathbf{U}_1$, etc. The Eq.(15) gives a combination of rotations on the Poincaré sphere with random axes given by matrices $\mathbf{U}_i$, but having the same rotation angles proportional to $\delta\omega$. Thus, the total rotation will be a realization of a "random walk". In a limited frequency range, while $\delta\omega$ is small enough, the single rotation around a fixed axis and constant angular velocity can be associated with a matrix product. As the rotation axis is random, the frequency range for this behavior if N is big, is inversely proportional to the square root of the number of matrices multiplied, i.e to the fiber length. Out of this range, the differential delay and polarization state become incorrelated. The short pulse which has a wide spectrum can be represented as a coherent superposition of pulses, which are long enough to behave as a whole. Since different long pulses have uncorrelated phases, their superposition will produce a pattern which has high contrast. The theory of such superposition is well known for the

spatial analog of pulse propagation. It describes the optical speckle [11]. Thus, we will refer to the general behavior as a "speckled pulse" or "temporal speckle". The width of individual speckle is determined by a maximal difference in frequencies, *i.e.* in our content it is of an order of the initial pulse width. The particular shape of pattern can be expected to vary strongly with slight changes in fiber environment.

The simulation presented in Fig.3 illustrates the point. For this, we have numerically calculated a product of the type Eq.(15) for 300 pieces, taking a randomly chosen unitary $\mathbf{U}_i$ matrix at every step. The initial pulse was chosen as having the uniform spectrum in a limited frequency range, which gives $sin(t)/t$ pulse amplitude in a time domain. Every individual realization has a speckled structure, but averaging over a big number of such realizations, one gets a Gaussian-shaped curve. Thus, if polarization mode dispersion is the only factor (there is no normal one), for an individual pulse one does not get a smooth curve, but a temporal speckle having a Gaussian-shape envelope. The action of PMD on the coherent pulse is qualitatively different from the action of normal dispersion, though if one averages over realizations, both types of dispersion have identical influence.

5. Conclusions

In conclusion, we have shown that the efficient perturbation technique can be applied for polarization evolution in fibers. The approximation validity range has an order of the beatlength for perturbation. In birefringent fibers with random additions to polarization and twist, spatial harmonics which add to the spatial frequency of the beatlength of the main part of birefringence contribute to the trajectory spreading over the Poincaré sphere. The rest of perturbation harmonics produce on the sphere a small-amplitude "jitter". Thus, the spreading has clear resonance character.
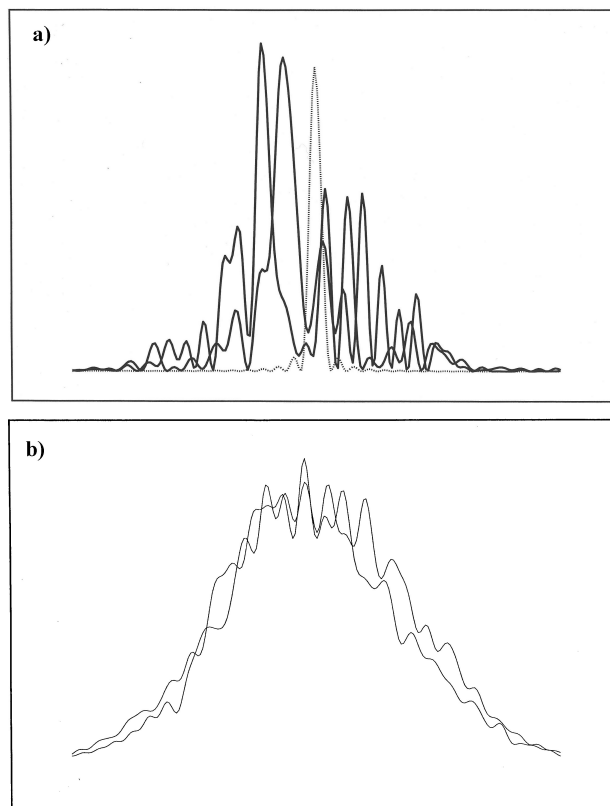

FIGURE 3 Influence of polarization mode dispersion on the short coherent pulse without taking the normal dispersion into account. a) The dashed line is the initial pulse shape. The solid lines are pulse shapes in two orthogonal polirization modes after propagation (normalized for better visibility). b) The average of the output pulse shape taken over 100 random realizations of the fiber.

The diagram technique permits to relate realistic perturbation statistics to the parameters of the widely used coarse step method of modeling. We also demonstrate that a developed polarization mode dispersion results for coherent pulses in a pulse splitting, and formation of a temporal speckle structure.

1. I.P.Kaminow, *IEEE J.Quantum Electon.* **QE-17** (1981) 15.

2. L.F.Mollenauer, K.Smith, J.P.Gordon, C.R.Menyuk, *Opt.Lett.* **14** (1989) 1219.

3. A.O.Dal Forno, A.Paradisi, J.P. von der Weid, *IEEE Phot.Tech.Lett.*, **12** (2000) 296.

4. A.Caltarossa, L.Palmieri, M.Schiano, T.Tambosso, *Opt.Lett.* **25** (2000) 384.

5. A.Iserles, S.P.Nørsett, *Philosophical transactions. math., phys.* **357** (1999) 983.

6. W.Magnus, *Comm.Pure & Appl. Math.* **7** (1954) 649.

7. R.Gilmore, *Lie groups, Lie algebras and some of their applications* (Wiley, New York, 1974).

8. C.R.Menyuk and P.K.A.Wai, *JOSA B* **11** (1994) 1288.

9. C.D Poole and R.E.Wagner, *Electron. Lett.* **22** (1986) 1029.

10. G.J.Foschini and C.D Poole, *J. Lightwave Technol.* **9** (1991) 1439.

11. J.W.Goodman, *Statistical Optics* (Wiley, New York, 1985).